Fast route to equilibration

Roie Dann [1,3,*] Ander Tobalina,[2,3,†] and Ronnie Kosloff [1,3,‡]
[1]*Institute of Chemistry, Hebrew University of Jerusalem, Jerusalem 9190401, Israel*
[2]*Department of Physical Chemistry, University of the Basque Country UPV/EHU, Apdo 644, Bilbao, Spain*
[3]*Kavli Institute for Theoretical Physics, University of California, Santa Barbara, California 93106, USA*

(Received 12 December 2019; accepted 13 April 2020; published 4 May 2020)

We present a control scheme for quantum systems coupled to a thermal bath. We demonstrate state-to-state control between two Gibbs states. This scheme can be used to accelerate thermalization and cool the open system. Starting from a microscopic description, we derive the reduced system dynamics, leading to a nonadiabatic master equation. The equation contains nontrivial effects due to the nonadiabatic driving and bath interaction. These special features enable controlling the open system and accelerating the entropy changes. For a two-level system model, we obtain a general solution and introduce a reverse-engineering scheme for control. The control problem is analyzed in the context of the theory of quantum control and the accompanying thermodynamic cost.

DOI: 10.1103/PhysRevA.101.052102

I. INTRODUCTION

Thermalization, the dynamical approach of a system towards thermal equilibrium, is of the utmost importance in contemporary physics. Typically, thermalization occurs once a system interacts with a large thermal reservoir of a defined temperature. In the quantum world, this dynamical process is embedded in the theory of open quantum systems and is consistent with the laws of thermodynamics [1].

In present-day quantum physics, thermalization is commonly employed to initialize a system state before further manipulations are preformed. For example, the initialization step in circuit quantum computing is a thermalization step and adiabatic quantum computing relies completely on thermalization to carry out a computation protocol [2–4]. In these examples, experimenters utilize the system-bath interaction to reduce the system temperature, suppressing the effective number of quantum states. Time-domain pump-probe spectroscopy relies on thermalization to close the loop of repeated experiments [5]. Moreover, thermalization is a vital step in quantum heat engines, and its timescale dictates the power output of the device [6–11].

Typically, thermalization is treated as a passive process. An interaction between a nonequilibrium system and the environment is introduced, and the thermal temperature of the environment and the system-bath coupling dictate the typical relaxation timescale. Moreover, after the initial thermalization step, the experimenter usually invests a considerable effort in isolating the system from environmental effects to attenuate the relaxation rate. In contrast to these approaches, the present study aims to harvest the environmental interactions to actively control the system and accelerate the thermalization.

Quantum control relies on the interference of pathways to achieve the control objective. Such interference requires a nonstationary superposition of states, i.e., quantum coherence. Commonly, coupling to a thermal bath causes decoherence, which tends to suppress the ability to control. Conversely, in the presented scheme, this interplay between coherence generation by the controller and decoherence by the bath will be shown to enable control.

We addressed this issue in a short letter [12]: *Shortcut to Equilibrium* (STE), where we described a procedure inducing swift thermalization by a rapid change in the system Hamiltonian. The process was demonstrated for a parametric harmonic oscillator coupled to a bath, and later combined with unitary strokes to study quantum analogues of the Carnot cycle at finite time [13]. In the current paper, we present a comprehensive account of the fast thermalization process. We emphasize the relation between quantum control and quantum thermodynamics, employing the thermalization of a qubit as our primary example. This allows for a detailed thermodynamics account of the related cost of rapid thermalization. We further extend the control scheme to include an initial nonequilibrium Gibbs state and a protocol that cools the system below the temperature of the bath. In addition, we elaborate on the connection to quantum coherent control.

The paper is organized as follows: we set the control framework and objective in Sec. II. Section III presents a first-principle analysis of the open system dynamics. We begin by solving for the propagator of the isolated system utilizing the inertial theorem, then include a weak interaction between the system and the bath, and present a brief construction of the nonadiabatic master equation (NAME). Following the dynamical construction, Sec. IV analyzes the task of rapid thermalization within the framework of quantum control theory. Section V constructs the dynamical description of a two-level system coupled to a thermal bath, demonstrating the general derivation. Next, we solve the two-level system dynamics and discuss its properties. Following the solution, we present a reverse-engineering control scheme to obtain a STE

*roie.dann@mail.huji.ac.il
†ander.tobalina@ehu.eus
‡kosloff1948@gmail.com

protocol that induces rapid thermalization. Generalizations of the scheme are considered, including an initial nonequilibrium Gibbs state and a target state which is colder than the bath. Section VI is devoted to results and discussion. We conclude in Sec. VII with a summary and discuss relevant implications and future prospects.

II. CONTROL OBJECTIVE AND FRAMEWORK

We aim to find a rapid thermalization protocol of a subsystem S coupled to a bath. This can be generalized to state-to-state control from an initial Gibbs state $\rho_S^i = \frac{1}{Z_{S,i}} \exp[-\beta_i \hat{H}_S(t_i)]$ with Hamiltonian $\hat{H}_S(t_i) = \hat{H}_S^i$ and inverse temperature β_i, toward the target state $\hat{\rho}_S^f = \frac{1}{Z_{S,f}} \exp[-\beta_f \hat{H}_S(t_f)]$ with a final Hamiltonian $\hat{H}_S(t_f) = \hat{H}_S^f$ and inverse temperature β_f. This objective falls into the category of state-to-state control of open quantum systems [14].

The control framework lies in a composite Hilbert space partitioned into a system and a bath. The combined system's evolution is governed by the total Hamiltonian

$$\hat{H}(t) = \hat{H}_S(t) + \hat{H}_B + \hat{H}_I, \tag{1}$$

where $\hat{H}_S(t)$ is the time-dependent system Hamiltonian which includes the external driving. $\hat{H}_B$ is the bath Hamiltonian, and $\hat{H}_I$ is the system-bath interaction term. To proceed, we make three basic assumptions:

(a) Only the system Hamiltonian is controllable, via external driving

(b) The bath is sufficiently large to maintain a thermal state at all times

(c) The system bath coupling is weak (and given *a priori*).

A solution for the control problem consists of two major steps: first, obtaining accurate reduced dynamical equations of motion for the system variables; second, finding a framework where the control problem can be solved parametrically, based on the equations of motion.

III. DRIVEN DYNAMICS OF THE OPEN SYSTEM

To achieve control, we require a dynamical equation of motion for a nonadiabatically driven system coupled to a bath. We employ a derivation based on first principles which complies with thermodynamic principles. The reduced dynamics is then formulated by a completely positive trace-preserving map, generated by the Gorini-Kossakowski-Lindblad-Sudarshan (GKLS) master equation [15,16]:

$$\frac{d}{dt}\hat{\rho}_S(t) = -\frac{i}{\hbar}[\hat{H}_S(t), \hat{\rho}_S(t)] + \mathcal{L}_D(t)\hat{\rho}_S(t), \tag{2}$$

where $\mathcal{L}_D$ is the dissipative part. The main issue lies in the fact that the dissipative part in the equations of motion depends on the system Hamiltonian and is therefore influenced by the driving. Neglecting this contribution leads to inconsistencies with thermodynamics [1].

A. Inertial solution of the free dynamics

An accurate description of the open system dynamics requires, first, an explicit solution of the free dynamics $\mathcal{U}_S(t)$. Obtaining such a solution is difficult when the free Hamiltonian does not commute at different times $[\hat{H}_S(t), \hat{H}_S(t')] \neq 0$. In this case, there is no common basis that diagonalizes $\mathcal{U}_S(t)$. A formal solution is given by a time-ordering procedure,

$$\mathcal{U}_S(t) = \overleftarrow{\mathcal{T}} \exp\left\{-i\int_0^t [\hat{H}_S(t'), \bullet]\, dt'\right\}, \tag{3}$$

where $\overleftarrow{\mathcal{T}}$ is the chronological time-ordering operator. However, this solution contains an infinite sum and is therefore impractical for our purposes. An explicit solution requires bypassing the time-ordering obstacle. This is achieved by utilizing the inertial theorem and solution. The inertial solution is a consequence of the theorem; it approximates the system dynamics under the condition of slow acceleration of the drive [17].

The proof of this property is established in the framework of the Liouville space representation and assumes a system with a closed Lie algebra. Liouville space is a Hilbert space of system operators, endowed with an inner product $(\hat{A}, \hat{B}) \equiv \mathrm{tr}(\hat{A}^\dagger \hat{B})$ [5,18,19]. In this space, the quantum system is represented in terms of a finite operator basis. These operators form a vector $\vec{v}$ in Liouville space. The operator dynamics are calculated using the Heisenberg equation, and for a closed operator algebra, the dynamical equations are cast in a matrix vector form:

$$\frac{d\vec{v}(t)}{dt} = -i\mathcal{M}(t)\vec{v}(t). \tag{4}$$

Here $\mathcal{M}(t)$ is the dynamical generator in Liouville space. For a varying Hamiltonian the generator has an explicit time dependence.

The inertial theorem relies on *a priori* decomposition of $\mathcal{M}(t)$ into a time-dependent scalar function $\Omega(t)$ and a constant matrix $\mathcal{B}(\vec{\chi})$, dependent on constants $\{\chi_i\}$, written in short notation as $\vec{\chi} = \{\chi_1, \chi_2, \ldots, \chi_m\}^T$:

$$\mathcal{M}(t) = \Omega(t)\mathcal{B}(\vec{\chi}). \tag{5}$$

Such a decomposition is achieved by expressing the Liouville dynamics in terms of a suitable time-dependent operators basis $\vec{v}(t) = \{\hat{v}_1(t), \ldots, \hat{v}_N(t)\}^T$ and control protocol $\hat{H}_S(t)$.

Combining Eqs. (4) and (5) and diagonalizing $\mathcal{B}$, we find the eigenvectors $\{\vec{F}_k\}$ of $\mathcal{U}_S(t) = \exp[-i\mathcal{B}\int_0^t \Omega(t')\,dt']$. These Liouville vectors define the eigenoperators, $\{\hat{F}_k\}$, of the free propagator (free w.r.t. the system-bath coupling), according to the mapping $\hat{F}_k = \sum_{i=1}^N f_i \hat{v}_i$, where f_i and $\hat{v}_i$ are the elements of $\vec{F}_k$ and $\vec{v}$. The set of eigenoperators forms a basis in Liouville space and satisfies an eigenvalue-type equation,

$$\hat{F}_k(\vec{\chi}, t) = \hat{U}_S^\dagger(t)\hat{F}_k(\vec{\chi}, 0)\hat{U}_S(t) = e^{-i\lambda_k\theta(t)}\hat{F}_k(\vec{\chi}, 0), \tag{6}$$

where $\hat{U}_S(t)$ is the free propagator in the Schrödinger representation, and λ_k is the kth eigenvalue of $\mathcal{B}$ and $\theta(t) = \int_0^t \Omega(t')\,dt'$.

Equations (5) and the associated solution (6) assumed a constant $\{\chi_i(t)\}$, we now generalize the solution to a slowly varying $\chi(t)$. When $(d\chi_i/d\theta \ll 1)$, the evolution of the eigenoperators is approximated by the inertial solution

$$\hat{F}_k(t) \equiv \hat{F}_k(\vec{\chi}(t), t) = e^{-i\int_{\theta(0)}^{\theta(t)} \lambda_k(\theta')\,d\theta'} e^{i\phi_k}\hat{F}_k(\vec{\chi}(t), 0). \tag{7}$$

Here $\lambda_k(\theta(t))$ are the instantaneous eigenvalues and ϕ_k is a geometrical phase [17]. Since $\{\hat{F}_k\}$ form a complete operator

basis, under the condition of a slow varying $\{\chi_i(t)\}$, Eq. (7) fully determines the system dynamics. Finally, we introduce the instantaneous diagonalization matrix $\mathcal{V}(\vec{\chi}(t))$ of $\mathcal{B}(\vec{\chi}(t))$ to obtain the inertial dynamics of the operators of $\vec{v}(t)$:

$$\begin{aligned}\hat{v}_i(t) &= \sum_{i,k} \mathcal{V}_{ik}\hat{F}_k(t) \\ &= \sum_{k} \mathcal{V}_{ik}(\vec{\chi}(t))e^{-i\int_{\theta(0)}^{\theta(t)}\lambda_k(\theta')\,d\theta'}\hat{F}_k(\chi(t),0) \\ &= \sum_{k,j} \mathcal{V}_{ik}(\vec{\chi}(t))e^{-i\int_{\theta(0)}^{\theta(t)}\lambda_k(\theta')\,d\theta'}\mathcal{V}^{-1}_{kj}(\vec{\chi}(t))\hat{v}_j(0). \end{aligned} \tag{8}$$

The solution is accurate under the condition that the inertial parameter is small:

$$\Upsilon = \sum_{n,k}\left|\frac{(\vec{G}_k, \vec{\nabla}_{\vec{\chi}}\mathcal{M}\vec{F}_n)}{(\lambda_n-\lambda_k)^2}\left(\frac{1}{\Omega}\frac{d\vec{\chi}}{dt}\right)^2\right|. \tag{9}$$

This occurs which for a slowly varying $\chi_i(t)$, when the eigenvalues λ_k and λ_n are distinct and Ω does is sufficiently large. The physical interpretation of a small inertial parameter roughly corresponds to moderate acceleration [17].

B. Construction of the NAME

We are now prepared to include the environmental influence and describe the dynamics of a nonadiabatically driven open quantum system. In this regime, when the typical driving timescale is comparable to the system Bohr frequencies $\Delta E/\hbar$, the external driving dresses the interaction with the bath. As a result, for fast driving, the adiabatic master equation [20–22] is inadequate [23].

To consistently describe the evolution of a nonadiabatically driven open quantum system, we construct the equation of motion utilizing a first-principle derivation. In the spirit of the Davis construction [24], we begin with a complete description of the composite system, Eq. (1), and assume weak-system-bath coupling. The complete dynamics is governed by the Liouville equation, which, within the Born-Markov approximation [25], leads to the Markovian quantum master equation

$$\frac{d}{dt}\tilde{\rho}_S(t) = -\frac{1}{\hbar^2}\int_0^\infty ds\ \mathrm{tr}_B[\tilde{H}_I(t),[\tilde{H}_I(t-s),\tilde{\rho}_S(t)\otimes\hat{\rho}_B]]. \tag{10}$$

Here $\tilde{\rho}_S(t) = \mathcal{U}_S(t)\hat{\rho}_S(t)$ is the reduced density matrix in the interaction representation, and a similar notation is applied for any system operator.

The interaction Hamiltonian can always be written as a sum of separable terms $\hat{H}_I = \sum_n \hat{S}_n\otimes\hat{B}_n$, where $\hat{S}_n$ and $\hat{B}_n$ are system and bath operators, respectively. Expressing the interaction term in terms of the operators $\hat{v}_i$, $\hat{S}_n = \sum_i s_{ni}\hat{v}_i(0)$ and assuming inertial driving, the inertial solution, Eq. (8), leads to

$$\begin{aligned}\tilde{H}_I(t) &= \sum_{n,k} c_{nk}(\vec{\chi}(t))e^{-i\int_{\theta(0)}^{\theta(t)}\lambda_k(\theta')\,d\theta'} \\ &\quad\times \hat{F}_k(\vec{\chi}(t),0)\otimes\tilde{B}_n(t) \\ &= \sum_{n,k}\xi_{nk}(\vec{\chi}(t))e^{-i\Lambda_{nk}(t)}\hat{F}_k(\vec{\chi}(t),0)\otimes\tilde{B}_n(t), \end{aligned} \tag{11}$$

with $\Lambda_{n,j}(t) \equiv \int_{\theta(0)}^{\theta(t)}\lambda_k(\theta')\,d\theta' + \eta_{nk}(t)$, where η_{nk} and ξ_{nk} are the phase and positive amplitude of $c_{nk}(\vec{\chi}(t)) = \sum_i s_{ni}\mathcal{V}^{-1}_{ik}(\vec{\chi}(t)) = \xi_{nk}(t)e^{-i\eta_{nk}(t)}$, respectively. Note that the Schrödinger and interaction pictures coincide when the operators are implicitly independent of time, $\tilde{F}_k(\vec{\chi}(t),0) = \hat{F}_k(\vec{\chi}(t),0)$.

Overall, the interaction term in the interaction representation is given as an expansion of the instantaneous eigenoperators $\hat{F}_k(\vec{\chi}(t),0)$, depending weakly on time through $\vec{\chi}(t)$. Now we substitute Eq. (11) into Eq. (10) and expand $\Lambda_{nk}(t-s)$ to first order in s near the instantaneous time t:

$$\Lambda_{nk}(t-s) \approx \Lambda_{nk}(t) - \frac{d\Lambda_{nk}(t)}{dt}s. \tag{12}$$

This approximation is justified if the bath dynamics are fast relative to the change in $\Lambda_{nk}(t)$, or alternatively, the change in the driving. In this regime, when s is comparable to, or greater than, the bath typical timescale, $s\sim\tau_B$, the contribution to the integral is negligible due to the fast decay of the bath correlation functions (Markovianity of the bath). In addition, from the inertial condition, the coefficients ξ_{nk} and eigenoperators $\hat{F}_k$ depend weakly on time [only through $\vec{\chi}(t)$], enabling the approximations $\xi(t-s)\approx\xi(t)$ and $\hat{F}_k(\vec{\chi}(t-s))\approx\hat{F}_k(\vec{\chi}(t))$. These approximations are justified for Markovian dynamics.

We now perform the rotating wave approximation, which eliminates nonconserving energy terms. Finally, in the spirit of Ref. [25] and neglecting the Lamb-shift term, the nonadiabatic master equation becomes

$$\begin{aligned}\frac{d}{dt}\tilde{\rho}_S(t) = \sum_k r_k[\hat{F}_k(\vec{\chi}(t))\tilde{\rho}_S(t)\hat{F}^\dagger_k(\vec{\chi}(t)) \\ - \{\hat{F}^\dagger_k(\vec{\chi}(t))\hat{F}_k(\vec{\chi}(t)),\tilde{\rho}_S(t)\}], \end{aligned} \tag{13}$$

with

$$r_k = \sum_{n,n'}\gamma_{nn'}(\Lambda'_{n,k}(t))\xi_{nk}(t)\xi_{n'k}(t),$$

where $\gamma_{nn'}(\alpha) = \int_{-\infty}^{\infty}ds\,e^{i\alpha s}\langle B^\dagger_n(s)B_{n'}(0)\rangle$ is the Fourier transformation of the bath correlation functions. The positivity of $\xi_{n,k}$ ensures that the NAME is of the GKLS form, guaranteeing a completely positive trace-preserving map [15,16]. For a more detailed derivation, see Ref. [23].

C. Validity regime of the NAME

The various approximations performed throughout the construction determine the validity regime of the final equation of motion. These approximations involve four timescales: (1) the system typical timescale $\tau_S\sim\omega^{-1}$, which is proportional to the inverse of the system's Bohr frequencies; (2) the timescale characterizing the decay of the bath correlation functions τ_B; (3) the system relaxation timescale, which scales with the square of the system-bath coupling constant, $\tau_R\propto g^2$, in the weak coupling limit; and (4) the driving timescale, identified as $\tau_d = \min_{n,k,t}\{[d\Lambda_{n,k}(t)/dt]/[d^2\Lambda_{n,k}(t)/dt^2]\}$.

Typically, master equations are valid under a coarse graining of time, neglecting memory effects within the bath relaxation time. Thermodynamically, such an approach is related to the isothermal partition of system and bath, and is valid in the weak coupling regime and manifested by the Born-Markov

approximation. Weak coupling between system and bath, $g \ll 1$, implies a slow relaxation relative to both system and bath internal dynamics, $\tau_R \gg \tau_S, \tau_B$. Moreover, the Born-Markov approximation is valid when the bath dynamics is much faster than the system dynamics, implying $\tau_B \ll \tau_S$. Following these approximations, fast oscillating phases are eliminated by the rotating wave approximation, which requires that $\tau_R \gg \tau_S$. Finally, the last assumption involves neglecting higher order terms in the expansion of $\Lambda(t-s)$ and $\xi(t-s)$. This assumption is justified when the bath correlation functions decay rapidly in comparison to the change in the driving, $\tau_B \ll \tau_d$.

The hierarchy between the four timescales determines the validity regime:

$$\tau_R \gg \tau_B, \quad \tau_S \gg \tau_B, \quad \tau_R \gg \tau_S, \quad \tau_d \gg \tau_B. \tag{14}$$

This implies that the NAME is exact in the weak coupling limit and a δ-correlated bath.

D. Eigenoperators connection to the Lindblad jump operators

The eigenoperators of the free evolution operator play a key role in the description of open quantum system dynamics. For example, according to the Davis construction [24] of the static master equation, population changes are induced by the ladder operators connecting energy eigenstates $|\varepsilon_k\rangle$ and $|\varepsilon_j\rangle$. As the Hamiltonian is time-independent, the eigenstates of the free propagator and the Hamiltonian coincide, and, as a result, the eigenoperators of the free propagator constitute the jump operators of the master equation. For a time-dependent Hamiltonian under periodic driving, the eigenoperators of the free propagator are the ladder operators between the Floquet states, which, according to a first-principle derivation, constitute the jump operators of the Floquet master equation [26].

These examples lead us to interpret the eigenoperators of the free evolution under nonadiabatic driving as the ladder operators of the associated "time-global" eigenstates, which account for the integration and time-ordering procedure in the free propagator. In fact, under nonadiabatic driving, the bath induces transformations with respect to those time-global states, and therefore, it is natural that the eigenoperators of the free propagator constitute the jump operators of the NAME.

E. Properties of nonadiabatic open system dynamics

Nonadiabatic features appear in the kinetic coefficients and Lindblad jump operators. Both depend on the driving protocol and differ from the equivalent terms in the adiabatic master equation [20,23]. These terms define an instantaneous attractor $\hat{\rho}_{I.A}$:

$$\mathcal{L}(t)\hat{\rho}_{I.A}(t) = 0. \tag{15}$$

This attractor is a generalized Gibbs state beyond the adiabatic limit. In general, any completely positive map has an invariant, which may not be unique [27]. Based on the Davis construction, where the invariant is the Gibbs state, we conjecture that for a nondegenerate Hamiltonian, the instantaneous attractor of the NAME is unique [1].

IV. QUANTUM CONTROL OF OPEN SYSTEMS

Fast thermalization can be formulated as a quantum control problem [14]. The task is classified as a state-to-state objective $\hat{\rho}_S^i \to \hat{\rho}_S^f$, governed by open system dynamics:

$$\frac{d}{dt}\hat{\rho}_S = \mathcal{L}(t)\hat{\rho}_S. \tag{16}$$

We consider a control problem where the reduced system dynamics is generated by the NAME [Eq. (13)].

Quantum control theory [14,28,29] addresses three main topics:

(1) Controllability, i.e., the conditions on the dynamics that allow obtaining the state-to-state objective

(2) Constructive mechanisms of control, the problem of synthesis

(3) Optimal control strategies and quantum speed limits.

These topics will be employed to analyze the process of fast thermalization.

A. State-to-state controllability

Under what conditions can an initial quantum state $\hat{\rho}_S^i$ be transformed into a final state $\hat{\rho}_S^f$, employing open systems dynamics? To prove controlability a single explicit solution for the control task is sufficient, under the dynamics of Eq. (16). In the context of the proof, the solution protocol has no time or energy restrictions. Entropy change is a necessary condition for open system controllability. This requirement leads to a natural decomposition of the protocol: an entropy-changing dissipative part followed by a fast unitary conserving entropy:

(a) For any initial state $\hat{\rho}_S^i$, couple the system to a bath of temperature T_B and change the Hamiltonian to $\hat{H}_S^f$ until it reaches an equilibrium thermal state $\hat{\rho}_{S,T_B}^f$, which has common eigenvalues with $\hat{\rho}_S^f$;

(b) Apply a fast unitary transformation $\hat{U}_S$, such that $\hat{\rho}_S^f = \hat{U}_S\hat{\rho}_{S,T_B}^f\hat{U}_S^\dagger$.

In the first stage, a dissipative transformation that leads to common eigenvalues with $\hat{\rho}_S^f$ is obtained by reaching a thermal state $\hat{\rho}_{S,T_B}^f = \sum \lambda_j|\phi_j\rangle\langle\phi_j|$, determined by the Hamiltonian: $\hat{H}_S^f = \sum_j \epsilon_j|\phi_j\rangle\langle\phi_j|$, where $\epsilon_j = kT(\log Z + \lambda_j)$. This state is unitarily equivalent to the target state, since unitary transformations do not alter the eigenvalues of the density matrix.

The protocol can be achieved under the following conditions:

(1) The isolated quantum system is completely unitary controllable, i.e., any unitary transformation $\hat{U}_S$ is admissible.

(2) There is a complete freedom in modifying the Hamiltonian $\hat{H}_S(t)$ of the system, embedded in the bath of temperature T_B.

The first controllability condition (1), open system entropy-changing control, can be addressed in the framework of the GKLS dynamical equations, Eq. (2). The control of a target state $\hat{\rho}_S^f$ requires engineering the asymptotic invariant of $\mathcal{L}$ to become unitarily equivalent to the target state [30–34]. In the adiabatic limit under the Davis construction, the thermal

state with the Hamiltonian $\hat{H}_S^f$ becomes the invariant of the GKLS equation [24].

The second condition, unitary control of a closed quantum system, is formulated employing a Lie algebra [28,35,36]. In this case, the Hamiltonian of the system is separated into drift and control terms,

$$\hat{H}_S(t) = \hat{H}_0 + \sum_j u_j(t)\hat{H}^j, \tag{17}$$

where $\hat{H}_0$ is the free system Hamiltonian, $u_j(t)$ are the control fields, and $\hat{H}_j$ are control operators. The system is unitary controllable provided that the Lie algebra, spanned by the nested commutators of $\hat{H}_0$ and $\hat{H}^j$, is full rank [28,35,36]. Under this condition, an arbitrary unitary propagator can be obtained. Such transformation necessarily preserves the eigenvalues of $\hat{\rho}_S$.

Controllability of open systems has previously been addressed assuming the dissipative generator $\mathcal{L}_D$, which is independent of the system Hamiltonian $\hat{H}_S$. This case has limited controllability [14,37,38], since there is no control of the invariant of $\mathcal{L}$. In the control community, the dependence of $\mathcal{L}$ on the Hamiltonian has been mostly overlooked (an exception is Ref. [39]). This dependence is required for a consistent thermodynamic description [1]. An exception arises for a singular bath (infinite temperature): then $\mathcal{L}_D$ is independent of $\hat{H}_S$ [40]. In this case the generator becomes $\mathcal{L}_D = -\gamma[\hat{G}, [\hat{G}, \bullet]]$. Then, if $\hat{G}$ belongs to the set of control operators (17), control is limited to a wedge in the state space [37]. A similar result is obtained if $\mathcal{L}_D$ is unital [41].

B. Constructive mechanisms of control

There are two limiting opposing mechanisms of control: adiabatic and quench. The adiabatic protocol interpolates between $\hat{H}_S^i$ and $\hat{H}_S^f$, implying the general form $\hat{H}_S(t) = \lambda(t)\hat{H}_S^i + [1-\lambda(t)]\hat{H}_S^f$, where $\lambda(t)$ is a slowly varying function of time. In this limit, the state remains in the canonical state $\hat{\rho}_S(t) = \frac{1}{Z}\exp[-\beta\hat{H}_S(t)]$, and no coherence is generated during the control procedure. This procedure is reversible, $\Delta\mathcal{S}_U = 0$, implying null dissipation of work $W_{\rm diss} = W - \Delta F_S = 0$, where ΔF_S is the change in free energy and $\mathcal{S}_U$ is the entropy of the universe. However, the optimal work cost, obtained in the adiabatic limit, is never practical since it requires an infinitely long execution time.

The other extreme mechanism is a quench: a sudden jump from the initial $\hat{H}_S^i$ to the target Hamiltonian $\hat{H}_S^f$, followed by a relaxation toward equilibrium [42]. Whenever $[\hat{H}_S^i, \hat{H}_S^f] \neq 0$ the protocol is irreversible. For such a case, the sudden quench generates significant coherence, requiring additional work that is eventually wasted by dissipation to the bath. This leads to an increased work cost, $W = \mathrm{Tr}\{\hat{\rho}_S^i(\hat{H}_S^f - \hat{H}_S^i)\}$, relative to the adiabatic work. The timescale of the quench protocol is dictated by the bath relaxation rates.

In the present study, we propose a fast control mechanism that serves as an intermediate between the adiabatic and sudden (quench) limits. In this protocol the state follows a generalized canonical form $\hat{\rho}_S(t) = \exp[\sum_j \lambda_j(t)\hat{A}_j]$, where λ_j are time-dependent coefficients and $\{\hat{A}_j\}$ are members of a closed Lie algebra which includes $\hat{H}_S(t)$. Asymptotically, for long protocol duration, this protocol converges to the adiabatic one. The fast protocol can achieve fast thermalization at low entropic cost. The basic idea, underlying the control scheme, is reverse engineering the control Hamiltonian $\hat{H}_S(t)$ such that a specific trajectory, defined by the generalized canonical form, is maintained.

C. Optimal control and quantum speed limit

Optimal control theory aims to find an accurate transformation of the system to the target state, subject to constraints of finite resources, such as time and external power. Optimal control algorithms have been applied to open system dynamics. Previously, in all cases studied, the dissipator $\mathcal{L}_D$ was independent of the control Hamiltonian $\hat{H}_S(t)$ [38,43–46]. An exception includes a time-dependent dissipator by utilizing the adiabatic master equation [47]. In the present study, we do not impose optimality; nevertheless, our fast thermalization protocol approximates the target. For the existing protocols, we can compare the actual protocol speed to theoretical bounds that limit the change in purity $P(t) = \mathrm{tr}[\hat{\rho}_S^2(t)]$ [48].

The speed limit of the purity change is given by

$$\left|\ln\left[\frac{P(t_f)}{P(t_i)}\right]\right| \leqslant 4\int_{t_i}^{t_f}\sum_k ||r_k(t')\hat{F}_k(t')||_{sp}^2\,dt, \tag{18}$$

where $\hat{F}_k$ and r_k are the Lindblad jump operators and rates, Eq. (13), and $||\cdot||_{sp}$ denotes the spectral norm. Many speed limits have been proposed [49–51], but the chosen one is specific for purity and is independent of the initial state.

V. SHORTCUT TO EQUILIBRIUM OF A TWO-LEVEL SYSTEM

We demonstrate the construction of a shortcut to equilibrium protocol for a two-level system embedded within a thermal bath. The general derivation follows the steps explicitly given in Sec. III. The first crucial step is to solve the free dynamics of the system, so as to obtain the propagator $\mathcal{U}_S(t)$.

A. Inertial dynamics of the isolated two-level system

We consider a two-level system (TLS) in the presence of two orthogonal modulated fields. The system is represented by the Hamiltonian

$$\hat{H}_S(t) = \omega(t)\hat{S}_z + \varepsilon(t)\hat{S}_x, \tag{19}$$

where $\hat{S}_i$, $i = x, y, z$ are the spin operators. Generally, the dynamics of a system with a time-dependent Hamiltonian is given by the time-ordered propagator, Eq. (3). However, this expression is only formal and is impractical for our analysis. We circumvent the time-ordering problem by utilizing the inertial theorem and solution [17].

The equations of motion for the $\mathfrak{su}(2)$ algebra can be cast into the desired form, Eq. (5), by choosing an appropriate time-dependent operators basis and protocol. To this end, we introduce two additional operators: $\hat{L}(t) = \varepsilon(t)\hat{S}_z - \omega(t)\hat{S}_x$ and $\hat{C}(t) = \bar{\Omega}(t)\hat{S}_y$, where $\bar{\Omega}(t) = \sqrt{\omega^2(t) + \varepsilon^2(t)}$ is the generalized Rabi frequency of the TLS, and define the Liouville

vector

$$\vec{v}(t) = \{\hat{H}_S(t), \hat{L}(t), \hat{C}(t)\}^T \quad . \tag{20}$$

Along with the identity $\hat{I}$, the elements of vector $\vec{v}(t)$ form a basis of the Liouville space, completely determining the system dynamics. For a protocol satisfying a constant adiabatic parameter for Eq. (19) [52] ($|\mu(t)| = \sum_{n\neq m} \frac{|\langle E_m(t)|\dot{\hat{H}}(t)|E_n(t)\rangle|}{[E_m(t)-E_n(t)]^2}$):

$$\mu \equiv \frac{\dot{\omega}\varepsilon - \omega\dot{\varepsilon}}{\bar{\Omega}^3}, \tag{21}$$

the dynamical equation in Liouville space is of the form $\frac{d\vec{v}}{dt} = [\frac{\dot{\bar{\Omega}}}{\bar{\Omega}^2}\mathcal{I} + \bar{\Omega}(t)\mathcal{B}(\mu)]\vec{v}$, where $\mathcal{I}$ is the identity matrix in Liouville space. Expressing the dynamics in terms of the scaled vector, $\vec{w}(t) \equiv \frac{\bar{\Omega}(0)}{\bar{\Omega}(t)}\vec{v}(t)$, leads to the required decomposition, Eq. (5), $\frac{d\vec{w}}{dt} = \mathcal{M}(t)\vec{w}$, with $\mathcal{M}(t) = \bar{\Omega}(t)\mathcal{B}(\mu)$. $\mathcal{B}(\mu)$ and the diagonalizing matrix $\mathcal{V}$ are given by

$$\mathcal{B}(\mu) = i\begin{bmatrix} 0 & \mu & 0 \\ -\mu & 0 & 1 \\ 0 & -1 & 0 \end{bmatrix}, \quad \mathcal{V} = \begin{bmatrix} 1 & -\mu & -\mu \\ 0 & i\kappa & -i\kappa \\ \mu & 1 & 1 \end{bmatrix}. \tag{22}$$

Such a solution contains a single constant parameter, $\vec{\chi} = \chi = \mu$.

Next, we utilize the inertial theorem to obtain the dynamics of the eigenoperators of the free propagators $\hat{F}_k = \{\hat{\xi}, \hat{\sigma}, \hat{\sigma}^\dagger\}$:

$$\begin{aligned} \hat{\xi}(\mu, 0) &= \frac{1}{\kappa\bar{\Omega}(0)}[\hat{H}_S(0) + \mu\hat{C}(0)] \\ \hat{\sigma}(\mu, 0) &= \frac{1}{2\kappa^2\bar{\Omega}(0)}[-\mu\hat{H}_S(0) - i\kappa\hat{L}(0) + \hat{C}(0)] \end{aligned} \tag{23}$$

and $\sigma^\dagger(\mu, 0)$, with corresponding eigenvalues $\lambda_1 = 0, \lambda_2(t) = \kappa(\mu(t))$ and $\lambda_3(t) = -\kappa(\mu(t))$, where

$$\kappa(\mu(t)) = \sqrt{1 + \mu^2(t)}. \tag{24}$$

For a slow change in μ the eigenoperators evolve according to the inertial solution $\vec{v}(t)$, with vector elements

$$\begin{aligned} \hat{v}_i(t) = \frac{\bar{\Omega}(t)}{\bar{\Omega}(0)} \sum_{j,k=1}^{3} \mathcal{V}_{ik}(\mu(t)) e^{-i\int_0^t \lambda_k(t')(\frac{d\bar{\theta}(t')}{dt'})\,dt'} \\ \times \mathcal{V}_{kj}^{-1}(\mu(t)\hat{v}_j(0)), \end{aligned} \tag{25}$$

with $\hat{F}_k(\mu(t), 0) = \mathcal{V}_{kj}^{-1}(\mu(t)\hat{v}_j(0))$ and $\bar{\theta}(t) = \int_0^t \bar{\Omega}(t')\,dt'$. The accuracy of the solution is given by the inertial parameter, Eq. (9), which for the TLS becomes

$$\Upsilon_{\mathrm{TLS}} = \frac{1}{2\kappa^2}\left(\frac{1}{\bar{\Omega}}\frac{d\mu}{dt}\right)^2. \tag{26}$$

When the inertial parameter is small ($\Upsilon \ll 1$), Eq. (25) describes the system dynamics accurately and is analogous to Eq. (8) of the general derivation.

To understand the practical implication of the inertial condition recall the role of the adiabatic parameter μ. This parameter naturally characterizes the qualitative accuracy of the adiabatic solution, evaluating the driving speed relative to the system Bohr frequencies. Hence, a slow change in μ corresponds to slow "acceleration" in the drive. Note that Eq. (25) is also valid for fast driving (nonadiabatic), with large μ, as along as the inertial condition is satisfied.

B. Inertial open system dynamics for the two-level system

For the studied example, we consider a system interacting with an ohmic boson bath at temperature T_B, through a single spin component

$$\hat{H}_I = g\hat{S}_y \otimes \hat{B}, \tag{27}$$

where $\hat{B}$ is the bath's interaction operator. Similarly, an alternative interaction can be assumed, leading to the same qualitative results. To derive the NAME we first perform a transformation to the interaction representation. This is achieved by noticing that $\hat{S}_y = \hat{C}(t)/\bar{\Omega}(t) = \hat{v}_3/\bar{\Omega}(t)$, and gathering Eqs. (23) and (25). Following the derivation described in Sec. III B, the explicit expression for $\tilde{H}_I(t)$ leads to a nonadiabatic master equation which is analogous to Eq. (13). The master equation for the two-level system reads

$$\begin{aligned} \frac{d}{dt}\tilde{\rho}_S(t) = k_\downarrow(t)\big[\hat{\sigma}(\mu)\tilde{\rho}_S\hat{\sigma}^\dagger(\mu) - \tfrac{1}{2}\{\hat{\sigma}^\dagger(\mu)\hat{\sigma}, \tilde{\rho}_S\}\big] \\ + k_\uparrow(t)\big[\hat{\sigma}^\dagger(\mu)\tilde{\rho}_S\hat{\sigma} - \tfrac{1}{2}\{\hat{\sigma}(\mu)\hat{\sigma}^\dagger(\mu), \tilde{\rho}_S\}\big], \end{aligned} \tag{28}$$

with kinetic coefficients

$$k_\uparrow(t) = \frac{2\alpha(t)}{\hbar c}N(\alpha(t)) = k_\downarrow(t)e^{-\alpha(t)/k_BT}, \tag{29}$$

$$\alpha(t) = \kappa(t)\bar{\Omega}(t), \tag{30}$$

and $\hat{\sigma}(\mu) \equiv \hat{\sigma}(\mu(t), 0)$ depends on the instantaneous adiabatic parameter $\mu(t)$. Equation (29) has a similar structure to the detailed balance relation exhibited in the adiabatic master equation [20]. However, beyond the adiabatic regime the transition frequency is increased by $\kappa(t)$, Eq. (30), which is always greater than unity, Eq. (24). This property is a consequence of the influence of the external driving on the dissipation.

C. Solution and properties of driven open systems

To solve the dynamics, we choose to parametrize the density operator as a generalized Gibbs state in a generalized canonical form

$$\tilde{\rho}_S(t) = Z^{-1}e^{\gamma(t)\hat{\sigma}(\mu)}e^{\beta(t)\hat{\xi}(\mu)}e^{\gamma^*(t)\hat{\sigma}^\dagger(\mu)}, \tag{31}$$

where $\tilde{Z} \equiv \tilde{Z}(t) = \mathrm{tr}(\tilde{\rho}_S(t))$ is the partition function, with time-dependent parameters $\gamma(t)$ and $\beta(t)$. Since $\{\hat{\xi}(\mu), \hat{\sigma}(\mu), \hat{\sigma}^\dagger(\mu), \hat{I}\}$ span the operator Hilbert space, Eq. (31) serves as a complete description of the TLS state. A linear parametrization is an additional option, leading to an alternative set of coupled equations [53].

Another common solution strategy is a formulation of the dynamics in the Heisenberg representation. However, when the Liouvillian $\mathcal{L}(t)$ (generator of the reduced open system dynamics) depends explicitly on time, as in Eq. (28), this framework requires a time ordering procedure [25].

To solve Eq. (31) we substitute Eq. (31) into Eq. (28) and obtain a set of coupled differential equations in terms of $\gamma(t)$

and ß(t):

$$\dot{ß} = \frac{\gamma e^{ß}}{2\kappa^2}\dot{\gamma}^* - k_\downarrow \frac{4\kappa^2(e^{ß}+1)+|\gamma|^2 e^{ß}}{16\kappa^4} + k_\uparrow \frac{(|\gamma|^2 + e^{-ß}4\kappa^2)[4(e^{ß}+1)\kappa^2 + e^{ß}|\gamma|^2]}{64\kappa^6} \quad (32)$$

$$\dot{\gamma} = k_\downarrow \frac{\gamma}{8\kappa^2} - k_\uparrow \frac{\gamma[2(1+2e^{-ß})\kappa^2 + |\gamma|^2]}{16\kappa^4}, \quad (33)$$

where the ß, γ, $k_\downarrow$, and $k_\uparrow$ are explicitly time-dependent and $\kappa(t)$ varies slowly with $\mu(t)$. These equations are an alternative representation of the open system dynamics.

The evolution is given in the interaction picture relative to the free dynamics. In this picture, the system rotates with the isolated driven system, so any change to the density operator is induced solely by the interaction with the bath.

D. Design of the control protocol

The driving generated by the control has both a direct impact on the state through the unitary part as well as an indirect influence through the dissipative part, Secs. III B and IV. To overcome this convoluted control scenario, we employ a reverse-engineering approach.

We consider the following control scenario. Initially, the system is in a Gibbs state, characterized by $\gamma(0) = 0$ with Hamiltonian $\hat{H}_S(0) = \hat{H}_S^i$ and temperature T_i. At the initial time, the system is coupled to a thermal bath of temperature T_B. We wish to construct a control protocol $\hat{H}_S(t)$ that drives the system to a Gibbs state at temperature T_f with the target Hamiltonian $\hat{H}_S(t_f) = \hat{H}_S^f$. In general, T_B, T_i, and T_f may differ from one another, that is, the initial and final states are not required to be in equilibrium with the bath, just in a Gibbs form. The assumption of an initial Gibbs state simplifies the analysis but does not modify the system's behavior qualitatively.

Since Eq. (33) vanishes when $\gamma(0) = 0$, the state conserves the form

$$\tilde{\rho}_S(t) = \tilde{Z}^{-1} e^{ß(t)\hat{\xi}(\mu)} \quad (34)$$

throughout its evolution, and the equation of motion is reduced to a single differential equation:

$$\dot{ß}(t) = \frac{1}{4\kappa^2[\mu(t)]}[k_\uparrow(t)(1+e^{-ß(t)}) - k_\downarrow(t)(e^{ß(t)}+1)]. \quad (35)$$

This equation is the basis for the suggested control scheme.

The control strategy is as follows. We perform a change of variables $y(t) = e^{ß(t)}$ and introduce a polynomial solution for $y(t)$ which satisfies the boundary conditions of the control. The initial and target Gibbs states correspond to values $ß(0) = -\hbar\bar{\Omega}_i/k_B T_i$ and $ß(t_f) = -\hbar\bar{\Omega}_f/k_B T_f$, where $\bar{\Omega}_i = \bar{\Omega}(0)$ and $\bar{\Omega}_f = \bar{\Omega}(t_f)$ are the generalized Rabi frequencies of the initial and final Hamiltonians, respectively. In addition, the values of $\dot{ß}(0)$ and $\dot{ß}(t_f)$ are set by Eq. (35) and the requirement of stationary control at the initial and final times, $\mu(0) = \mu(t_f) = 0$. Since the stationary condition implies $\dot{\alpha}(0) = \dot{\alpha}(t_f) = 0$, the second derivatives $\ddot{ß}(0)$ and $\ddot{ß}(t_f)$ are determined as well through the kinetic coefficients $k_\uparrow(\alpha(t))$, $k_\downarrow(\alpha(t))$, respectively [Eq. (29)].

TABLE I. Model parameters.

Coefficient	Value [atomic units]
Bath temperature	5
Coupling prefactor	$g^2/2\hbar c = 0.02$
Numerical integrating step	10^{-3}
Control parameters	$a = 10/t_f^2$ and $b = -2/3t_f$

A fifth-order polynomial for y is sufficient to satisfy the boundary condition of Eq. (35), leading to

$$ß(t) = \ln\left(\sum_{k=0}^{5} b_k t^k\right), \quad (36)$$

where the coefficients $\{b_k\}$ are presented in Table I. Next, we substitute the solution, Eq. (36), and the kinetic coefficients Eq. (29) into Eq. (35), which leads to an equation in terms of $\alpha(t)$. We solve for $\alpha(t)$ using a standard numerical solver. Finally, by numerically reversing Eq. (30), we obtain the control protocol $\bar{\Omega}(\alpha(t))$.

To gain some insight about the dynamics, we compute the instantaneous attractor of Eq. (35). The attractor $ß_{I.A}(t)$ is defined as the value of ß(t) for which $\dot{ß}(t) = 0$ [simply calculated by setting the LHS of Eq. (35) to zero]. When $ß(t) = ß_{I.A}(t)$, the system is stationary. As the dynamical map is a semigroup, the contraction property [54,55], implies that at each instant, the system propagates towards the instantaneous attractor state $\tilde{\rho}_S(ß_{I.A}(t))$.

For sufficiently slow driving, $\mu \ll 1$ (adiabatic regime), $\hat{\xi}(\mu(t))$ converges to the instantaneous Hamiltonian $\hat{H}_S(0)/\bar{\Omega}(0)$, and Eq. (35) describes a decay towards the adiabatic attractor, $ß_{I.A}(t) \to -\hbar\bar{\Omega}(t)/k_B T_B$. This means that at long times, the system state converges to the adiabatic result $\tilde{\rho}_S(t) = \exp\{-\hbar\bar{\Omega}(t)\hat{H}_S(0)/[\bar{\Omega}(0)k_B T_B]\}$. Moreover, in the adiabatic limit, the relaxation rate towards the instantaneous thermal state reduces to the adiabatic rate, $k = k_\downarrow^{\text{adi}} + k_\uparrow^{\text{adi}}$, where $k_{\downarrow,\uparrow}^{\text{adi}} = k_{\downarrow,\uparrow}(\bar{\Omega}(t))$, as $\alpha(t) \to \bar{\Omega}(t)$ [see Eq. (29)].

Conversely, beyond the adiabatic limit, $\mu \ll 1$, $\hat{\xi}(\mu(t))$ is a linear combination of $\hat{H}_S(0)$ and $\hat{C}(0)$ [see Eq. (23)]. As a result, the instantaneous attractor state is a rotated squeezed Gibbs state that differs from the instantaneous thermal state. Thus, due to the nonadiabatic driving, the map propagates the system toward a state that differs from equilibrium. Overall, this behavior can be understood as a dressing of the system by the drive, and consequently the bath interacts with a dressed system and leads the system toward the instantaneous attractor.

In practice, when $\mu \sim 1$, ß(t) does not vary sufficiently rapidly so to follow $ß_{I.A}(t)$. As a result, the system in the interaction picture remains a rotated squeezed Gibbs state with varying temperature throughout its evolution.

The relaxation rates are also altered by the nonadiabatic driving. Beyond the adiabatic regime they do not depend on the instantaneous generalized Rabi frequency, but on the effective frequency $\alpha(t)$ [Eq. (29)]. This leads to a skewed detailed balance and modifies the dissipation of energy and coherence.

The control protocol is defined in terms of the generalized Rabi frequency $\bar{\Omega}(t)$, leaving ambiguity concerning the values of $\omega(t)$ and $\varepsilon(t)$ [Eq. (19)]. For the current model, we choose

$$\omega(t) = \bar{\Omega}(t)\cos(\Phi(t)) \quad \text{and} \quad \varepsilon(t) = \bar{\Omega}(t)\sin(\Phi(t)), \quad (37)$$

where Φ is taken as a simple polynomial. Substituting Eq. (37) into μ, Eq. (21), leads to the relation $\dot{\Phi} = -\mu(t)\bar{\Omega}(t)$, which determines a solution of the form $\Phi(t) = a(t^2 + bt^3)$, satisfying the stationary condition at initial and final times. Here $b = -2/3t_f$ and a is a free parameter which should be sufficiently small to comply with the inertial condition $d\mu/dt \ll 2\kappa^2(d\theta/dt)$. For the modeling, it is chosen as $a = 10/t_f^2$, leading to $\mu \to 0$ for $t_f \to 0$.

VI. RESULTS AND DISCUSSION

A. Control

The control scheme allows addressing various control tasks:

(1) Transformation between two equilibrium states with different Hamiltonians (STE)

(2) Transformation between an initial nonequilibrium state to an equilibrium state, accompanied by a change in the Hamiltonian (STE)

(3) Transformation to a final state which is colder than the bath, $T_f < T_B$.

We study two classes of STE protocols, expansion and compression, with bath temperature $T_B = 5$. The expansion varies the generalized Rabi frequency from $\bar{\Omega}_i = 12$ to $\bar{\Omega}_f = 5$ (atomic units). Compression involves an increase in the generalized Rabi frequency: $\bar{\Omega}_i = 5 \to \bar{\Omega}_f = 12$. During the expansion (compression) protocols, the effective temperature $T_{\text{eff}} \equiv -\bar{\Omega}(t)/ß(t)$ decreases below (increases above) the bath temperature at transient times. At the final stage of the protocol, the effective temperature returns back to the bath temperature, and we obtain $T_{\text{eff}} = T_B$ at the final time (Fig. 1).

The shortcut to equilibrium protocols achieve high fidelity relative to the quench protocols for both expansion and compression procedures. Figure 2 shows the accuracy $\mathcal{A}$ of the target state for varying protocol duration. Within the inertial approximation the control is precise, and the fidelity $\mathcal{F}$ approaches unity. As a result, the inertial approximation is the limiting factor of the protocol accuracy. The fidelity is therefore evaluated by comparing the inertial solution for an isolated solution, under the shortcut protocol, to an exact numerical solution.

As the protocol duration increases, the inertial approximation improves, and the accuracy increases. In comparison, the quench protocol leads to slow relaxation toward equilibrium (Sec. IV B). Shortcut protocols show an improvement of up to fivefold in accuracy, relative to the quench procedure for the same protocol duration.

The accuracy of the compression protocol exceeds the expansion protocol (Fig. 2). This result stems from the difference in the energy gaps along the driving protocol $\bar{\Omega}(t)$ (see Fig. 4 below). As mentioned previously, the inertial approximation is the limiting factor of the protocol accuracy, and its accuracy improves as the inertial parameter Υ decreases. In the two-level system model, this parameter, Eq. (26),

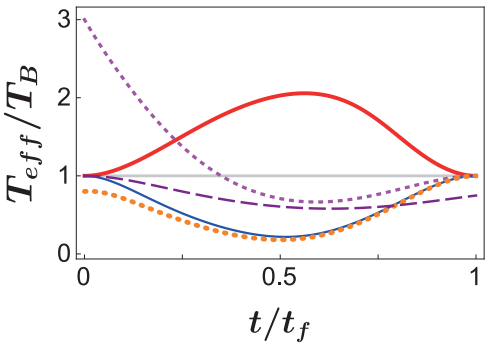

FIG. 1. Effective temperature as a function of time for protocol duration $t_f = 6\,(2\pi/\bar{\Omega}_{\text{ref}})$, for various STE protocols. The protocols are designated as follows: PE (continuous blue thin line), expansion with initial and final thermal states ($T_i = T_f = T = 5$); PC (continuous red thick line), compression with initial and final thermal states; PE1 (dashed light purple line), expansion initializing at a nonequilibrium Gibbs state, with temperature $T_i = 15$, with a final equilibrium state; PE2 (dashed orange thick line), expansion of an initial Gibbs state with $T_i = 4$ and a thermal target state $T_f = T = 5$; PEC (long-dashed dark purple line), expansion initializing at a thermal state with a final state colder than the bath, $T_f = 4$ (temperatures are given in atomic units). The gray continuous line designates $T_{\text{eff}} = T_B$, given as a reference.

$\Upsilon_{\text{TLS}} \propto \bar{\Omega}^{-2}$, leading to greater values of Υ_{TLS} during the expansion (involves smaller Rabi frequency values) relative to the compression process (involves larger Rabi frequency values).

The state trajectory in the $\{\hat{S}_x, \hat{S}_y, \hat{S}_z\}$ space (Fig. 3) displays the change in purity imposed by the control protocol: an increase of purity for compression and a decrease for expansion. The change in purity can be related to the speed

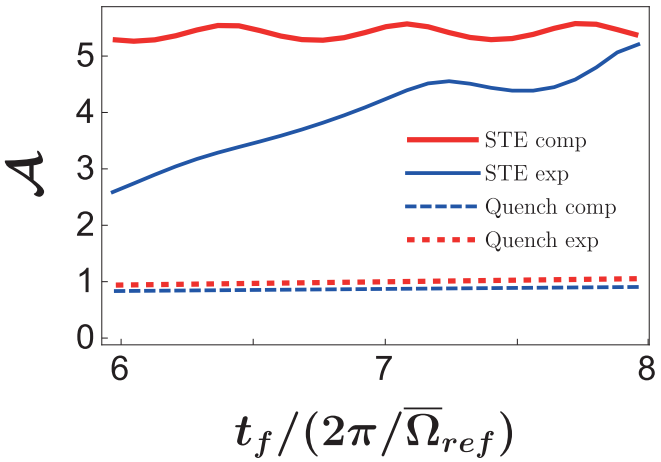

FIG. 2. Accuracy with respect to the control target as a function of protocol duration. The STE results correspond to expansion and compression protocols (PE and PC, respectively). These are compared to the analogous quench procedures. The accuracy is defined as $\mathcal{A} = -\log_{10}[1 - \mathcal{F}(\hat{\rho}_S(t_f), \hat{\rho}_{S,T})]$, and increases with the fidelity, given by $\mathcal{F}(\hat{\rho}_1, \hat{\rho}_2) = [\text{tr}(\sqrt{\sqrt{\hat{\rho}_1}\hat{\rho}_2\sqrt{\hat{\rho}_1}})]^2$ [56]. In the calculation, $\hat{\rho}_S(t_f)$ accounts for the deviations from the inertial approximation. The reference Rabi frequency is given by $\bar{\Omega}_{\text{ref}} = 5$ a.u.

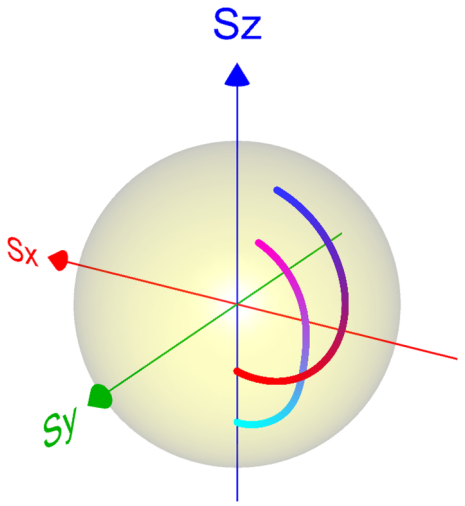

FIG. 3. Two-level system trajectory in the spin operator space $\{\langle\hat{S}_x\rangle, \langle\hat{S}_y\rangle, \langle\hat{S}_z\rangle\}$. The surface of the sphere represents states with purity of 1, while the center of the sphere represent a fully mixed state. The compression trajectory (PC), red to blue (initializes on the $\hat{S}_z$ axis), increases the purity (initially closer to the center of the sphere and propagates towards the surface of the sphere), and the expansion trajectory (PE), cyan to purple, decreases it (initially on the $\hat{S}_z$ axis closer to the surface and propagates towards the center of the sphere).

limit [Eq. (18)]; the bound on the purity change, for expansion and compression, is 1.58, while the STE protocols yield a value of 0.34. This value shows that although the STE is not optimum, its nevertheless within the range of the speed limit.

The dynamics are imposed by nontrivial protocols (Fig. 4) of $\omega(t)$ and $\varepsilon(t)$. These time-dependent frequencies are a single option from a family of procedures that correspond to the protocol $\bar{\Omega}(t)$ (see Sec. V D).

We find that the different protocols of compression and expansion for various initial states (Gibbs states with different temperatures) are all characterized by overshoot relative to the target frequency. As seen in Fig. 4, the expansion protocol [reduction in the generalized Rabi frequency $\bar{\Omega}(t)$] achieves values above the target frequency, whereas the compression first increases $\bar{\Omega}$, before a fast decline to $\bar{\Omega}(t_f)$. A similar behavior was witnessed for the STE protocol for a Harmonic oscillator [12]. Formally, this behavior is connected to the proposed ansatz, Eq. (36), and a different ansatz may alter this result. Nevertheless, this outcome fits the need to generate coherence, which in turn allows controlling the energy via a unitary transformation.

The STE protocol can be employed for an initial nonequilibrium Gibbs state. For example, expansion protocols PE1 and PE2 begin in a Gibbs state with $T_i \neq T_B$ (see Figs. 1 and 4). These STE protocols induce an energy exchange with the bath that leads the state toward an equilibrium state, with $T_{\text{eff}}(t_f) = T_B$. The fidelity of protocols PE1 and PE2 are comparable to those of PE and PC (see Fig. 1 and Table II).

Cooling is demonstrated in Fig. 1, where the system reaches a final temperature of $T_f = 4$ a.u., below the bath temperature T_B. The final state is unstable once the driving ceases, that is, if the system remains in contact with the bath,

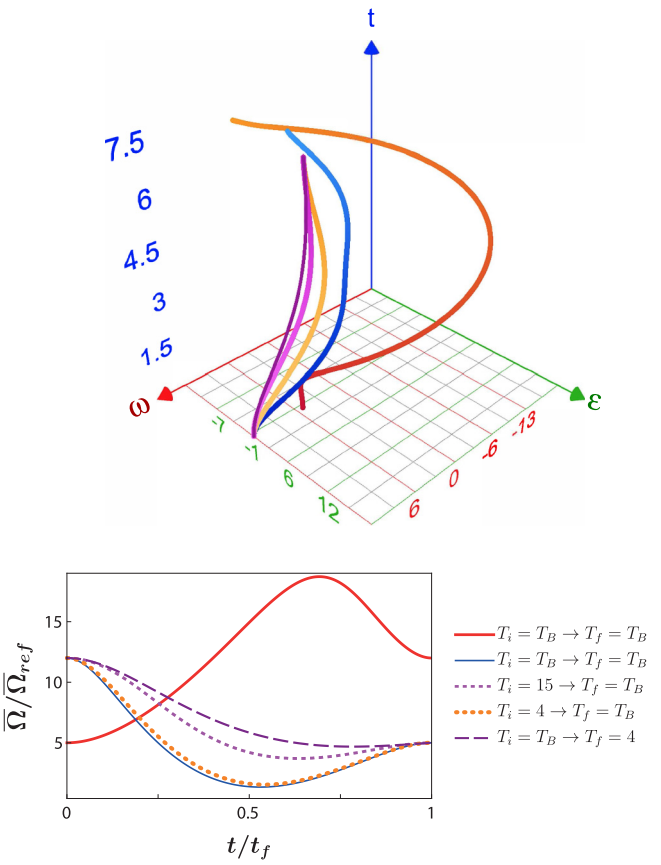

FIG. 4. Top: frequencies $\omega(t)$ and $\varepsilon(t)$, Eq. (19), as a function of time for expansion and compression protocols. The expansion protocols initialize at $\omega = 12$ a.u. and $\varepsilon = 0$ a.u., while the compression starts at $\omega = 5$ a.u. with $\varepsilon = 0$ a.u. $[\Omega(t) = \sqrt{\omega^2(t) + \varepsilon^2(t)}]$. The various protocols differ by their initial temperature. Bottom: generalized Rabi frequency as a function of time for protocol duration $t_f = 6\,(2\pi/\bar{\Omega}_{\text{ref}})$, where $\bar{\Omega}_{\text{ref}} \equiv 5$ a.u.. Both expansion (continuous blue thin line, PE) and compression (continuous red thick line, PC) protocols show an overshoot with respect to the final Rabi frequency. The STE protocols and color code correspond to Fig. 1.

it will equilibrate. The effect is shown in Fig. 8 below. We find that this control task is sensitive to the protocol, and further analysis is required in order to map the accessible cooling regime.

TABLE II. Typical protocols for state-to-state transformations in atomic units. All procedures were performed employing a thermal bath with temperature $T = 5$. $\bar{\Omega}_i$ and $\bar{\Omega}_f$ are the initial and final generalized Rabi frequencies of the TLS, respectively. The initial and final Gibbs state temperatures are T_i and T_f.

Label	$\bar{\Omega}_i$	$\bar{\Omega}_f$	T_i	T_f
PE (Expansion)	5	12	5	5
PC (Compression)	12	5	5	5
PE1	5	12	15	5
PE2	5	12	4	5
PEC	5	12	5	4

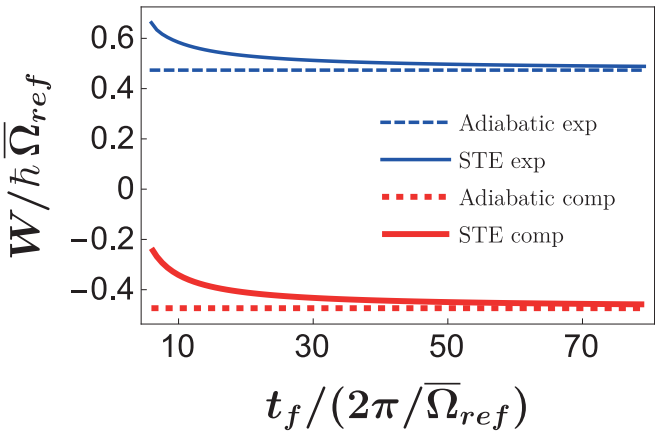

FIG. 5. Work as a function of the protocol duration t_f for expansion, the two blue thin lines (PE), and compression, the two red thick lines (PC), STE procedures. Optimal values, obtained in the adiabatic limit ($t_f \to \infty$), appear as dashed lines. Equilibration acceleration is accompanied by a work cost relative to the adiabatic result. This leads to an increased work cost for compression protocols and reduced work extraction during expansion.

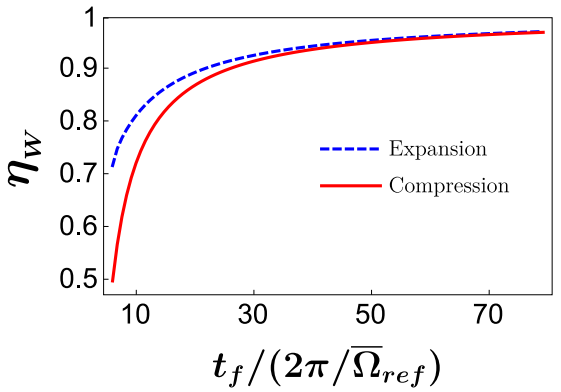

FIG. 6. Efficiency as a function of the protocol duration t_f for expansion (dashed-blue, PE) and compression (continuous red, PC) STE procedures. Color codes are defined in Fig. 1.

B. Thermodynamic analysis

The manipulation of a system Hamiltonian by external fields has an associated work cost or gain (gain or extracted work is considered a negative work cost). This cost can be connected to quantum friction [9,57], which implies that faster transformations are accompanied by a higher energy cost [58–62]. We identify this cost with the microscopic work, defined as the time integral over the instantaneous power $\mathcal{P}(t) \equiv \langle \frac{\partial \hat{H}_S(t)}{\partial t} \rangle$. This interpretation is motivated by the correspondence between work and energy for an isolated system. In the absence of environmental interactions, the change in the system's energy can be formulated as $\Delta E_S(t) = \int_0^t \mathcal{P}(t')\,dt' = W$, utilizing the Heisenberg picture for an isolated system. An extended definition also accounts for the cost of the external controller [63]. This additional cost requires an explicit description of the controller, which is beyond the scope of this study.

From conservation of energy, heat is then determined as $Q = \Delta E_S - W$, with $\Delta E_S = \mathrm{tr}(\hat{H}_S(t_f)\hat{\rho}_S(t_f)) - \mathrm{tr}(\hat{H}_S(0)\hat{\rho}_S(0))$. Utilizing the linearity of integration and the trace, this relation becomes $Q = \int_0^t \mathcal{J}(t')\,dt'$, where $\mathcal{J}(t') \equiv \mathrm{tr}(\hat{H}_S(t')\frac{d}{dt'}\hat{\rho}_S(t'))$ is the heat current.

The shortcut procedures accelerate the thermalization rate by investing additional work. Compared to the adiabatic protocol, the STE harvests less work in extraction (compression for the TLS) and requires an additional work cost under expansion (Fig. 5) [64]. The additional cost can be traced back to the transformation of invested work to coherence, which is then dissipated to the bath. As the protocol duration increases, coherence generation is suppressed, and the STE work cost converges to the adiabatic result. To evaluate the relative performance, we define the work efficiency η_W, for an expansion of the two-level system $\eta_W = W_{\mathrm{adi}}/W$, and for compression $\eta_W = W/W_{\mathrm{adi}}$, where W_{adi} is the adiabatic work. For fast protocols $t_f \sim 6\,(2\pi/\bar{\Omega}_{\mathrm{ref}})$, the work efficiency gives values of $\eta_W = 0.71$ for expansion and $\eta_W = 0.5$ for compression (see Fig. 6). For larger protocol duration, the work efficiency improves in accordance with the work.

The expansion protocol exhibits an improved efficiency relative to the compression protocol. This result is a consequence of the two different STE driving protocols: the expansion protocol [the continuous blue (lower) line in Fig. 4] includes a moderate overshoot relative to the lower final frequency, leading to a slower drive, while the compression protocol includes a strong overshoot to high frequencies [the continuous red (upper) line]. This overshoot requires faster driving and, therefore, generates significant coherence and demands a considerable greater work input relative to the ideal adiabatic protocol. In addition, increasing the frequency gap relative to the target frequency enhances the dissipation. As a result, a large amount of coherence and energy dissipates, leading to a reduced efficiency with respect to the expansion protocol.

When the open quantum system, initially at thermal equilibrium, expands heat flows from the bath to the system, increasing its entropy. Figure 7 shows the increase in the system's von Neumann entropy $\mathcal{S}_{V.N}$ along the expansion protocol, accompanied by a reduction in the bath entropy $\mathcal{S}_B = -\mathcal{Q}/T_B$. Their sum gives the total change in the entropy of the universe $\mathcal{S}_U$, which is strictly positive for any irreversible process. As expected, the fast driving during the STE protocol induces irreversible dynamics that increases $\mathcal{S}_U$.

To evaluate the coherence generation, we compare $\mathcal{S}_{V.N}$ and energy entropy $\mathcal{S}_E = -k_B \sum_i p_i \ln p_i$, where $\{p_i\}$ are the populations in the energy representation. As seen in Fig. 7, the two are very close, demonstrating that for protocol duration $t_f = 6\,(2\pi/\bar{\Omega}_{\mathrm{ref}})$, the dynamics is dominated by the energy. Nevertheless, the two entropies differ at intermediate times when the state exhibits maximal coherence. At the beginning and final times $\mathcal{S}_{V.N} = \mathcal{S}_E$, since the state is diagonal in the energy representation.

Another measure of the irreversibility is the entropy production Σ. Close to equilibrium, it can be defined as $\Sigma = \mathcal{S}_{V.N} - \mathcal{Q}/T_B$ or equivalently, as $W - \Delta F_S$. For the general case, the quantum entropy production rate is recognized with the negative derivative of the Kullback-Leibler diver-

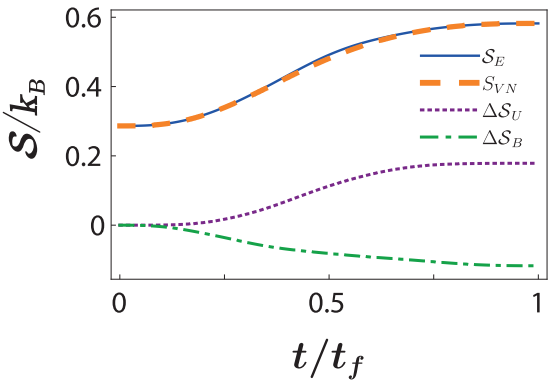

FIG. 7. Entropy as a function of time for an expansion procedure (PE) with protocol duration $t_f = 6\,(2\pi/\bar{\Omega}_{\rm ref})$. $\Delta\mathcal{S}_B$ is the change in the entropy of the bath, due to heat transfer. $\mathcal{S}_{VN}$ is the von Neumann entropy of the system; the change in the entropy of the universe is $\Delta\mathcal{S}_U$ and $\mathcal{S}_E$ is the system's energy entropy. $\mathcal{S}_E$ always exceeds the von Neumann entropy because it does not contain information about the quantum correlations between the energy states.

gence [25] between the system state and the fixed point of the dynamical map (the instantaneous attractor). The divergence is a measure of the difference between two quantum states $\mathcal{D}(\hat{\rho}_1||\hat{\rho}_2) = \mathrm{tr}(\hat{\rho}_1(\ln\hat{\rho}_1 - \ln\hat{\rho}_2))$. It is non-negative, and it decreases as the system evolves under Eq. (2) [27]. This property implies the positivity of the entropy production rate $\dot{\Sigma}(\hat{\rho}_S(t)) \equiv -\frac{d}{dt}\mathcal{D}(\hat{\rho}_S(t)||\hat{\rho}_S^{I,A}) \geqslant 0$. Figure 8 presents the entropy production rate during a STE expansion protocol. As expected the entropy production rate is positive. It reaches maximum values at intermediate times, when coherence builds up and dissipates to the bath. This dissipation leads to the increase in total entropy and irreversibility. When the

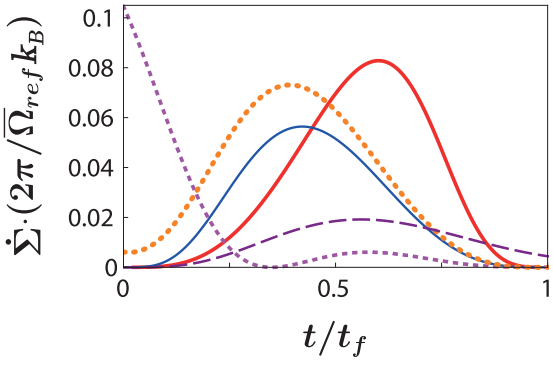

FIG. 8. Entropy production rate as a function of time for protocol duration $t_f = 6\,(2\pi/\bar{\Omega}_{\rm ref})$. Continuous red thick (right peak) and blue thin (left peak) curves correspond to expansion and compression procedures, respectively, with initial and final thermal states. When the system is in equilibrium with the bath, the entropy production vanishes ($t = 0$ and $t = t_f$ for these protocols). Notice that the cooling protocol (long dashed dark purple line) has a final positive entropy production rate as the system is in a nonequilibrium Gibbs state ($T_f = 4 \neq T_B$). The dashed orange thick and dashed light purple thin lines are associated with initial nonequilibrium Gibbs states; orange and light purple dashed lines correspond to $T_i = 4$ and $T_f = 15$ (atomic units), respectively.

initial or final states are not in equilibrium with the bath (procedures PE1, PE2, and PEC), the entropy production does vanish at corresponding boundary.

The cooling mechanism is analogous to that of a power driven refrigerator, where the two-level system mimics a cold bath with finite heat capacity. The driving supplies the power to pump heat from the cold bath and dump it into the hot bath. In such a cooling scenario, consistency with thermodynamics requires a positive entropy production and investment of work. This is verified in Fig. 8.

VII. CONCLUSIONS

Thermalization is typically considered a spontaneous process, the rate of which is determined by the system-bath coupling strength. We demonstrated that thermalization can be actively controlled, resulting in acceleration of the thermalization rate. Our control is achieved by implementing external driving that modifies the system Hamiltonian directly. First principle treatment (Sec. III) showed that the time dependence of the system Hamiltonian dresses the system-bath interaction, modifying the dissipative part indirectly. This structure is vital for a dynamical description that complies with thermodynamic principles [1]. The dissipative part adjusts to the change in the Hamiltonian and is therefore indirectly controlled.

Alternatively, direct control over dissipation can be obtained in the "singular bath limit," i.e., an additional δ-correlated noisy driving with a fast timescale with respect to all other considered timescales [65]. In this case the dissipation is independent of the system Hamiltonian. A recent study showed that a Langevin-type term, rising from momentum kicks, can lead to acceleration of the thermalization rate [66]. Moreover, an additional suggestion concerns the reset of a qubit, assumes a supply of cold ancilla qubits, and engineers the reset by applying two qubit gates [67]. Another suggestion, is to include a counterdiabatic term to engineer the Hamiltonian and dissipative part [68].

In a more generalized context, we incorporate the open-system control task into the theme of quantum control theory (Sec. IV). Adopting the principles of the themalization control scheme, the analysis led to the formal conditions of complete state-to-state controllablity of open systems (Sec. IV A).

Speeding up the themalization rate comes with a thermodynamic cost, with a minimum work cost achieved in the adiabatic limit. Any additional cost is associated with the emergence of friction. When the Hamiltonian does not commute with itself at different times, driving at nonvanishing speed generates coherence and is manifested by additional work which is dissipated to the bath. Dissipated energy heats the bath and leads to positive entropy production and irreversibility. The first-principle analysis conducted here demonstrated the quantum origin of friction.

To demonstrate the control scheme, we utilized a two-level-system model, characterized by an $\mathfrak{su}(2)$ algebra. Similarly, the analysis can be straightforwardly generalized to any system described by the same algebra and a Hamiltonian of the form of Eq. (19), such as the four-level system described in Refs. [9,69–71]. The present study originated from our previous analysis of the shortcut to equilibration (STE) of a harmonic oscillator [12]. These control schemes have

common properties: in both models, the fast protocols are characterized by overshoot with respect to the final control frequency. Furthermore, the thermodynamic cost shows a similar trend. In this study, we explored additional control protocols, extending the applicability of the control scheme. We showed that the control allows for nonequilibrium initial Gibbs states. Moreover, adding additional fast unitary transformations at initial and final times, allowed extending the control to a broad family of states containing the same initial and final entropies. Another surprising result is a protocol that leads to a final state that is colder than the bath ($T_f < T_B$). At first glance, this seems like a violation of thermodynamic principles, as it cannot be achieved under adiabatic driving. However, the fast driving generates conditions analogous to a power-driven refrigerator, where heat is pumped from the two-level-system to the thermal bath by consuming external power. The mechanism requires generation of coherence whose dissipation to the bath generates entropy, the latter compensating for the negative entropy change of the system. We emphasize that this cold state is transient.

Experimental realization of quantum heat engines has emerged recently [72]. The platform employed in these experiments includes various controlled quantum systems. The protocols introduced above can be directly employed in the current devices to realize quantum heat engines at finite times. In particular, these protocols can be used to realize a quantum Carnot engine with a qubit as a working medium [10].

A natural extension of the present study; would involve incorporating optimal control theory in the control of an open quantum system. The novelty of such an approach is the incorporation of control on the dissipation via external driving.

ACKNOWLEDGMENTS

We thank Christiane Koch for useful comments, and we thank KITP for their hospitality. This research was supported by the Adams Fellowship Program of the Israel Academy of Sciences and Humanities and the Israel Science Foundation, Grant No. 2244/14, the National Science Foundation under Grant No. NSF PHY-1748958, and the Basque Government under Grant No. IT986- 16 and MINECO/FEDER,UE and FIS2015-67161-P.

[1] R. Alicki and R. Kosloff, in *Thermodynamics in the Quantum Regime*, edited by F. Binder, L. Correa, C. Gogolin, J. Anders, and G. Adesso, Fundamental Theories of Physics Vol. 195 (Springer, Cham, 2018).
[2] P. Brooks and J. Preskill, Phys. Rev. A **87**, 032310 (2013).
[3] E. T. Campbell, B. M. Terhal, and C. Vuillot, Nature (London) **549**, 172 (2017).
[4] T. Albash, V. Martin-Mayor, and I. Hen, Phys. Rev. Lett. **119**, 110502 (2017).
[5] S. Mukamel, *Principles of Nonlinear Optical Spectroscopy* (Oxford University Press on Demand, New York, 1999).
[6] R. Alicki, J. Phys. A: Math. Gen. **12**, L103 (1979).
[7] E. Geva and R. Kosloff, J. Chem. Phys. **96**, 3054 (1992).
[8] R. Kosloff and Y. Rezek, Entropy **19**, 136 (2017).
[9] T. Feldmann and R. Kosloff, Phys. Rev. E **68**, 016101 (2003).
[10] D. von Lindenfels, O. Gräb, C. T. Schmiegelow, V. Kaushal, J. Schulz, M. T. Mitchison, J. Goold, F. Schmidt-Kaler, and U. G. Poschinger, Phys. Rev. Lett. **123**, 080602 (2019).
[11] J. P. Pekola, B. Karimi, G. Thomas, and D. V. Averin, Phys. Rev. B **100**, 085405 (2019).
[12] R. Dann, A. Tobalina, and R. Kosloff, Phys. Rev. Lett. **122**, 250402 (2019).
[13] R. Dann and R. Kosloff, New J. Phys. **22**, 013055 (2020).
[14] C. P. Koch, J. Phys.: Condens. Matter **28**, 213001 (2016).
[15] V. Gorini, A. Kossakowski, and E. C. G. Sudarshan, J. Math. Phys. **17**, 821 (1976).
[16] G. Lindblad, Commun. Math. Phys. **48**, 119 (1976).
[17] R. Dann and R. Kosloff, arXiv:1810.12094.
[18] T. Petrosky and I. Prigogine, *The Liouville Space Extension of Quantum Mechanics*, edited by I. Prigogine and S. A. Rice (John Wiley & Sons, New York, 1997).
[19] M. Am-Shallem, A. Levy, I. Schaefer, and R. Kosloff, arXiv:1510.08634.
[20] T. Albash, S. Boixo, D. A. Lidar, and P. Zanardi, New J. Phys. **14**, 123016 (2012).
[21] M. S. Sarandy and D. A. Lidar, Phys. Rev. A **71**, 012331 (2005).
[22] M. Yamaguchi, T. Yuge, and T. Ogawa, Phys. Rev. E **95**, 012136 (2017).
[23] R. Dann, A. Levy, and R. Kosloff, Phys. Rev. A **98**, 052129 (2018).
[24] E. B. Davies, Commun. Math. Phys. **39**, 91 (1974).
[25] H.-P. Breuer and F. Petruccione, *The Theory of Open Quantum Systems* (Oxford University Press on Demand, Oxford, 2002).
[26] R. Alicki, D. Gelbwaser-Klimovsky, and G. Kurizki, arXiv:1205.4552.
[27] G. Lindblad, Commun. Math. Phys. **40**, 147 (1975).
[28] D. d'Alessandro, *Introduction to Quantum Control and Dynamics* (Chapman and Hall/CRC, Boca Raton, Florida, 2007).
[29] S. J. Glaser, U. Boscain, T. Calarco, C. P. Koch, W. Köckenberger, R. Kosloff, I. Kuprov, B. Luy, S. Schirmer, T. Schulte-Herbrüggen, D. Sugny, and F. K. Wilhelm, Eur. Phys. J. D **69**, 279 (2015).
[30] S. Lloyd and L. Viola, Phys. Rev. A **65**, 010101(R) (2001).
[31] N. Lütkenhaus, J. I. Cirac, and P. Zoller, Phys. Rev. A **57**, 548 (1998).
[32] K. W. Murch, U. Vool, D. Zhou, S. J. Weber, S. M. Girvin, and I. Siddiqi, Phys. Rev. Lett. **109**, 183602 (2012).
[33] R. Puthumpally-Joseph, O. Atabek, E. Mangaud, M. Desouter-Lecomte, and D. Sugny, Mol. Phys. **115**, 1944 (2017).
[34] J. Fischer, D. Basilewitsch, C. P. Koch, and D. Sugny, Phys. Rev. A **99**, 033410 (2019).
[35] G. M. Huang, T. J. Tarn, and J. W. Clark, J. Math. Phys. **24**, 2608 (1983).
[36] V. Jurdjevic and H. J. Sussmann, J. Diff. Equ. **12**, 313 (1972).
[37] G. Dirr, U. Helmke, I. Kurniawan, and T. Schulte-Herbrüggen, Rep. Math. Phys. **64**, 93 (2009).

[38] V. Mukherjee, A. Carlini, A. Mari, T. Caneva, S. Montangero, T. Calarco, R. Fazio, and V. Giovannetti, Phys. Rev. A **88**, 062326 (2013).
[39] D. D'Alessandro, E. Jonckheere, and R. Romano, in *Proceedings of the 21st Symposium Math. Theory of Networks and Systems* (University of Groningen, Groningen, Netherlands, 2014), pp. 1677–1684.
[40] V. Gorini and A. Kossakowski, J. Math. Phys. **17**, 1298 (1976).
[41] C. O'Meara, G. Dirr, and T. Schulte-Herbruggen, IEEE Tran. Automatic Control **57**, 2050 (2012).
[42] H. Quan and W. H. Zurek, New J. Phys. **12**, 093025 (2010).
[43] A. Bartana, R. Kosloff, and D. J. Tannor, J. Chem. Phys. **106**, 1435 (1997).
[44] A. Bartana, R. Kosloff, and D. J. Tannor, Chem. Phys. **267**, 195 (2001).
[45] Y. Ohtsuki, W. Zhu, and H. Rabitz, J. Chem. Phys. **110**, 9825 (1999).
[46] O. V. Morzhin and A. N. Pechen, Lobachevskii J. Math. **40**, 1532 (2019).
[47] D. Basilewitsch, F. Cosco, N. L. Gullo, M. Möttönen, T. Ala-Nissilä, C. P. Koch, and S. Maniscalco, New J. Phys. **21**, 093054 (2019).
[48] R. Uzdin and R. Kosloff, Europhys. Lett. **115**, 40003 (2016).
[49] D. P. Pires, M. Cianciaruso, L. C. Céleri, G. Adesso, and D. O. Soares-Pinto, Phys. Rev. X **6**, 021031 (2016).
[50] L. Mandelstam and I. Tamm, in *Selected Papers*, edited by B. M. Bolotovskii, V. Ya. Frenkel, and R. Peierls (Springer, Berlin, 1991), pp. 115–123.
[51] N. Margolus and L. B. Levitin, Physica D **120**, 188 (1998).
[52] A. Messiah, *Quantum Mechanics* (Elsevier, Amsterdam, 1981), Vol. 2.
[53] R. Kosloff and T. Feldmann, Phys. Rev. E **82**, 011134 (2010).
[54] J. A. Goldstein, Semigr. Forum **23**, 375 (1981).
[55] A. Pazy, *Semigroups of Linear Operators and Applications to Partial Differential Equations*, Applied Mathematical Sciences Vol. 44 (Springer Science & Business Media, Berlin, 2012).
[56] A. Uhlmann, Rep. Math. Phys. **9**, 273 (1976).
[57] F. Plastina, A. Alecce, T. J. G. Apollaro, G. Falcone, G. Francica, F. Galve, N. LoGullo, and R. Zambrini, Phys. Rev. Lett. **113**, 260601 (2014).
[58] X. Chen and J. G. Muga, Phys. Rev. A **82**, 053403 (2010).
[59] K. Hoffmann, P. Salamon, Y. Rezek, and R. Kosloff, Europhys. Lett. **96**, 60015 (2011).
[60] P. Salamon, K. H. Hoffmann, Y. Rezek, and R. Kosloff, Phys. Chem. Chem. Phys. **11**, 1027 (2009).
[61] S. Campbell and S. Deffner, Phys. Rev. Lett. **118**, 100601 (2017).
[62] D. Stefanatos, IEEE Trans. Autom. Control **62**, 4290 (2017).
[63] A. Tobalina, I. Lizuain, and J. Muga, Europhys. Lett. **127**, 20005 (2019).
[64] Unlike typical working mediums, work is extracted from the TLS in a compression process and invested under expansion.
[65] S. Schirmer, E. Jonckheere, S. O'Neil, and F. C. Langbein, in *Proceedings of the 2018 IEEE Conference on Decision and Control (CDC)* (IEEE, Piscataway, NJ, 2018), pp. 6608–6613.
[66] L. Dupays, I. Egusquiza, A. del Campo, and A. Chenu, arXiv:1910.12088.
[67] D. Basilewitsch, J. Fischer, D. M. Reich, D. Sugny, and C. P. Koch, arXiv:2001.09107.
[68] S. Alipour, A. Chenu, A. T. Rezakhani, and A. del Campo, arXiv:1907.07460.
[69] R. Kosloff and T. Feldmann, Phys. Rev. E **65**, 055102(R) (2002).
[70] D. Türkpençe and F. Altintas, Quantum Inf. Proc. **18**, 255 (2019).
[71] H.-P. Peng, M.-F. Fang, M. Yu, and H.-M. Zou, Int. J. Theor. Phys. **57**, 1872 (2018).
[72] J. Ronagel, S. T. Dawkins, K. N. Tolazzi, O. Abah, E. Lutz, F. Schmidt-Kaler, and K. Singer, Science **352**, 325 (2016).